## 2.6 Actuator Dynamics

We have discussed the dynamics of a rigid-robot manipulator in joint space and Cartesian coordinates. However, the robot needs actuators to move it; these are generally either electric or hydraulic motors. It is now required, therefore, to add the actuator dynamics to the arm dynamics to obtain a complete dynamical description of the arm plus actuators. A good reference on actuators and sensors is provided by [de Silva 1989].

### Dynamics of a Robot Arm with Actuators

We shall consider the case of electric actuators, assuming that the motors are armature controlled. Hydraulic actuators are described by similiar equations. In this subsection we suppose that the armature inductance is negligible.

The equations of the $n$-link robot arm from Table 2.3-1 are given by

$$M(q)\ddot{q} + V_m(q,\dot{q})\dot{q} + F(\dot{q}) + G(q) = \tau, \qquad (2.6\text{-}1)$$

where $q \in \mathbb{R}^n$ is the arm joint variable. The dynamics of the armature-controlled dc motors that drive the links are given by the $n$ decoupled equations

$$J_M\ddot{q}_M + B\dot{q}_M + F_M + R\tau = K_M v, \tag{2.6-2}$$

where $q_M = \text{vec}\{q_{Mi}\} \in \mathbb{R}^n$, with $q_{Mi}$ the $i$th rotor position angle and $\text{vec}\{a_i\}$ denoting a vector with components $a_i$. The control input is the motor voltage vector $v \in \mathbb{R}^n$.

The actuator coefficient matrices are all constants given by

$$\begin{aligned} J_M &= \text{diag}\{J_{Mi}\} \\ B &= \text{diag}\{B_{Mi} + K_{bi}K_{Mi}/R_{ai}\} \\ R &= \text{diag}\{r_i\} \\ K_M &= \text{diag}\{K_{Mi}/R_{ai}\}, \end{aligned} \tag{2.6-3}$$

where the $i$th motor has inertia $J_{Mi}$, rotor damping constant $B_{Mi}$, back emf constant $K_{bi}$, torque constant $K_{Mi}$, and armature resistance $R_{ai}$.

The gear ratio of the coupling from the $i$th motor to the $i$th arm link is $r_i$, which we define so that

$$q_i = r_i q_{Mi} \qquad \text{or} \qquad q = Rq_m. \tag{2.6-4}$$

If the $i$th joint is revolute, then $r_i$ is a dimensionless constant less than 1. If $q_i$ is prismatic, then $r_i$ has units of m/rad.

The actuator friction vector is given by

$$F_M = \text{vec}\{F_{Mi}\}$$

with $F_{Mi}$ the friction of the $i$th rotor.

Note that capital "$M$" denotes motor constants and variables, while $V_m$ is the arm Coriolis/centripetal vector defined in terms of Christoffel symbols.

Using (2.6-4) to eliminate $q_M$ in (2.6-2), and then substituting for $\tau$ from (2.6-1) results in the dynamics in terms of joint variables

$$(J_M + R^2M)\ddot{q} + (B + R^2V_m)\dot{q} + (RF_M + R^2F) + R^2G = RK_M v \tag{2.6-5}$$

or, by appropriate definition of symbols,

$$(M'(q)\ddot{q} + V'(q,\dot{q})\dot{q} + F'(\dot{q}) + G'(q) = K'v. \tag{2.6-6}$$

**Properties of the Complete Arm-Plus-Actuator Dynamics.** The complete dynamics (2.6-6) has the same form as the robot dynamics (2.6-1). It is very easy to verify that the complete arm-plus-actuator dynamics enjoys the same properties as the arm dynamics that are listed in Table 2.3-1 (see the Problems). In particular, $V'$ is one-half the difference between $\dot{M}'$ and a skew-symmetric matrix, all the boundedness assumptions hold, and linearity in the parameters holds. Thus, in future work where we design controllers, *we may assume that the actuators have been included in the arm equation in Table 2.3-1.*

**Independent Joint Dynamics.** In many commercial robot arms the gear ratios $r_i$ are very small, providing a large torque advantage in the actuator/link coupling. This has important ramifications that greatly simplify the design of robot arm controllers.

To explore this, let us write the complete dynamics by components as

$$(J_{Mi} + r_1^2 m_{ii})\ddot{q}_i + B_i\dot{q}_i + r_i F_{Mi} = \frac{r_i K_{Mi}}{R_{ai}} v_i - r_i^2 \mathrm{d}_i, \qquad i = 1, \ldots, n, \quad (2.6\text{-}7)$$

where $B \equiv \mathrm{diag}\{B_i\}$ and $d_i$ is a disturbance given by

$$d_i = \sum_{j \neq i} m_{ij}\ddot{q}_j + \sum_{j,k} V_{jki}\dot{q}_j\dot{q}_k + F_i + G_i \quad (2.6\text{-}8)$$

with $m_{ij}$ the off-diagonal elements of $M'$, $V_{jki}$ the tensor components of $V'\dot{q}$, $F_i$ the friction of the $i$th link, and $G_i$ the $i$th gravity component.

This equations reveals that if $r_i$ is small, the arm dynamics are approximately given by *n decoupled second-order equations with constant coefficients.* The dynamical effects of joint coupling and gravity appear only as disturbance terms multiplied by $r_i^2$. That is, robot controls design is virtually the problem of simply *controlling the actuator dynamics.*

Unfortunately, modern high-performance tasks make the Coriolis and centripetal terms large, so that $d_i$ is not small. Moreover, modern high-performance arms have near-unity gear ratios (e.g., direct drive arms), so that the nonlinearities must be taken into account in any conscientious controls design.

## Third-Order Arm-Plus-Actuator Dynamics

An alternative model of the complete robot arm is sometimes used in controls design [Tarn et al. 1991]. It is a third-order differential equation that should be used when the motor armature inductance is not negligible.

When the armature inductances $L_i$ are not negligible, instead of (2.6-2) we must use the armature-controlled dc motor equations

$$TK_M'\dot{I} + K_M'I + B'\dot{q}_M = K_M v \quad (2.6\text{-}9)$$

$$J_M\ddot{q}_M + B_M\dot{q}_M + F_M + R\tau = K_m'I \quad (2.6\text{-}10)$$

with $I \in \mathbb{R}^n$ the vector of armature currents,

$$\begin{aligned} T &= \mathrm{diag}\{L_i/R_{ai}\} \\ K_m' &= \mathrm{diag}\{K_{Mi}\} \\ B' &= \mathrm{diag}\{K_{bi}K_{Mi}/R_{ai}\} \\ B_M &= \mathrm{diag}\{B_{Mi}\}. \end{aligned} \quad (2.6\text{-}11)$$

It is important to note that $T$ is a matrix of motor electric time constants. In the preceding subsection, these time constants were assume negligibly small in comparison to the motor mechanical time constants.

To determine the overall dynamics of the arm plus dc motor actuators, eliminate $\tau$ between (2.6-1) and (2.6-10) to obtain an expression for $I$. Then, differentiate to expose explicitly $\dot{I}$. Substitute these expressions into (2.6-9) (see the Problems) to obtain dynamics of the form

$$D\frac{d^3}{dt^3}q + f(q,\dot{q},\ddot{q}) = RK_M v. \tag{2.6-12}$$

The coefficient matrix $D$ is given by

$$D(q) = TM'(q), \tag{2.6-13}$$

so that it is negligible when $L_i$ are small.

## Dynamics with Joint Flexibility

We have assumed that the coupling between between the actuators and the robot links is provided through rigid gear trains with gear ratios of $r_i$. In actual practice, the coupling suffers from backlash and gear train flexibility or elasticity. Here we include the flexibility of the joints in the arm dynamic model, assuming for simplicity that $r_i = 1$.

This is not difficult to do. Indeed, suppose that the coupling flexibility is modeled as a stiff spring. Then the torque mentioned in equations (2.6-1), (2.6-2) is nothing but

$$\tau = B_s(\dot{q}_M - \dot{q}) + K_s(q_M - q), \tag{2.6-14}$$

with $B_s = \text{diag}\{b_{si}\}$, $K_s = \text{diag}\{k_{si}\}$, and $b_{si}$ and $k_{si}$ the damping and spring constants of the $i$th gear train. Thus the dynamical equations become

$$M(q)\ddot{q} + V_m(q,\dot{q})\dot{q} + F(\dot{q}) + G(q) + B_s(\dot{q} - \dot{q}_M) + K(q - q_M) = 0 \tag{2.6-15}$$

$$J_M\ddot{q}_M + B\dot{q}_M + F_M + B_s(\dot{q}_M - \dot{q}) + K(q_M - q) = K_M v. \tag{2.6-16}$$

The structure of these equations is very different from the rigid joint arm described in Table 2.3-1. We discuss the control of robot manipulators with joint flexibility in Chapter 6 (see [Spong 1987]). The next example shows the problems that can occur in controlling flexible joint robots.

### EXAMPLE 2.6-1: DC Motor with Flexible Coupling Shaft

To focus on the effects of joint flexibility, let us examine a single armature-controlled dc motor coupled to a load through a shaft that has significant flexibility. The electrical and mechanical subsystems are shown in Fig. 2.6-1.

The motor electrical equation is

$$L\dot{i} = -Ri - k_m'\dot{\theta}_m + u \tag{1}$$

with $i(t)$, $u(t)$ the armature current and voltage, respectively. The back emf is $v_b = k_m'\dot{\theta}_m$.

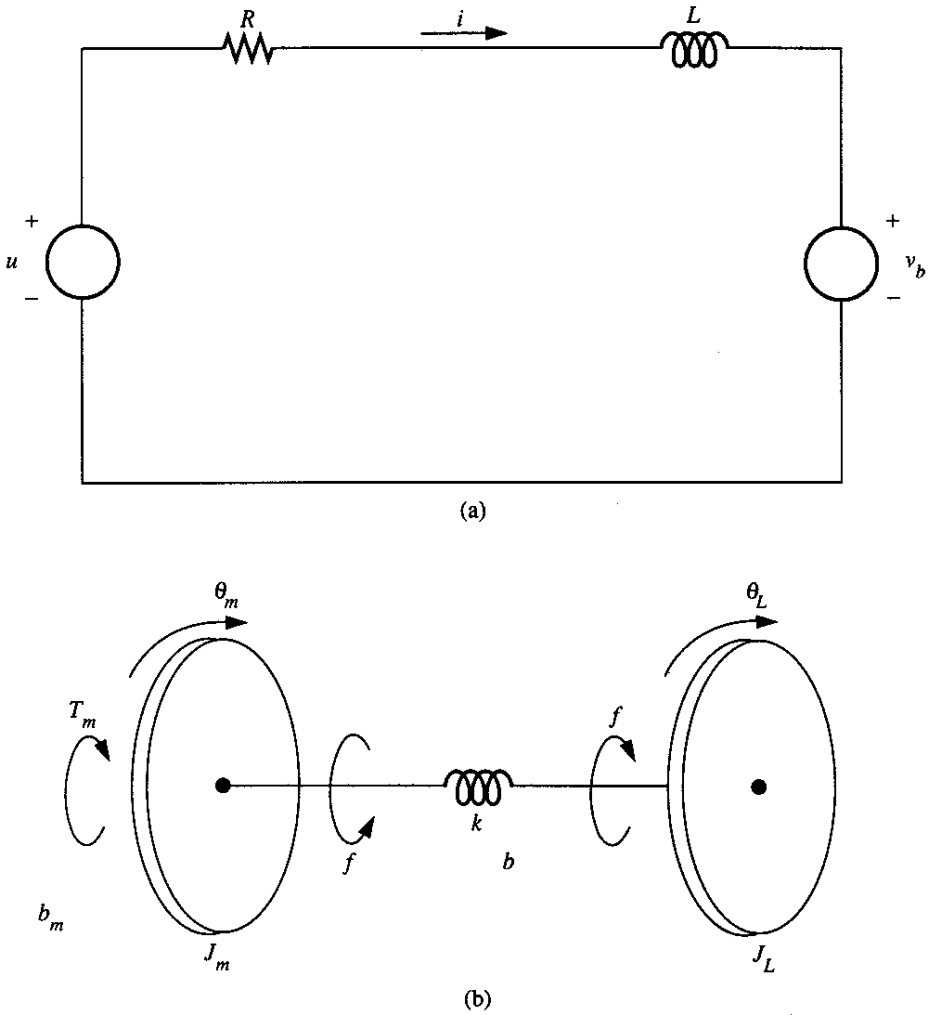



**FIGURE 2.6-1** Dc motor with shaft compliance: (a) electrical subsystem; (b) mechanical subsystem.

The interaction force exerted by the flexible shaft is given by $f = b(\dot{\theta}_m - \dot{\theta}_L) + k(\theta_m - \theta_L)$, where the shaft damping and spring constants are denoted by $b$ and $k$. Thus the mechanical equations of motion may be written down as

$$J_m\ddot{\theta}_m + b_m\dot{\theta}_m + b(\dot{\theta}_m - \dot{\theta}_L) + k(\theta_m - \theta_L) = k_m i \tag{2}$$

$$J_L\ddot{\theta}_L + b(\dot{\theta}_L - \dot{\theta}_m) + k(\theta_L - \theta_m) = 0, \tag{3}$$

with subscripts $m$ and $L$ referring, respectively, to motor parameters and load parameters. The load inertia $J_L$ is assumed constant. The definitions of the remaining symbols may be inferred from the foregoing text.

To place these equations into state-space form, define the state as

$$x = [i \quad \theta_m \quad \omega_m \quad \theta_L \quad \omega_L]^T, \tag{4}$$

with $\omega_m = \dot{\theta}_m$ and $\omega_L = \dot{\theta}_L$ the motor and load angular velocities. Then

$$\dot{x} = \begin{bmatrix} \frac{-R}{L} & 0 & \frac{-k_m'}{L} & 0 & 0 \\ 0 & 0 & 1 & 0 & 0 \\ \frac{k_m}{J_m} & \frac{-k}{J_m} & \frac{-(b+b_m)}{J_m} & \frac{k}{J_m} & \frac{b}{J_m} \\ 0 & 0 & 0 & 0 & 1 \\ 0 & \frac{k}{J_L} & \frac{b}{J_L} & \frac{-k}{J_L} & \frac{-b}{J_L} \end{bmatrix} x + \begin{bmatrix} \frac{1}{L} \\ 0 \\ 0 \\ 0 \\ 0 \end{bmatrix} u. \tag{5}$$

### a. Rigid Coupling Shaft

If there is no compliance in the coupling shaft, $\omega_m = \omega_L \equiv \omega$ and the state equations reduce to (see the Problems)

$$\dot{x} = \begin{bmatrix} -R/L & -k_m'/L \\ k_m/J & -b_m/J \end{bmatrix} x + \begin{bmatrix} 1/L \\ 0 \end{bmatrix} u \equiv Ax + Bu, \tag{6}$$

where $x = [i \quad \omega]^T$, $J = J_m + J_L$. Defining the output as the motor speed gives

$$y = [0 \quad 1]x \equiv Cx.$$

The transfer function is computed to be

$$H(s) = C(sI - A)^{-1}B = \frac{k_m}{(Ls + R)(Js + b_m) + k_m k_m'}. \tag{7}$$

Using parameter values of $J_m = J_L = 0.1$ kg-m$^2$, $k_m = k_m' = 1$ V-s, $L = 0.5$ H, $b_m = 0.2$ N-m/rad/s, and $R = 5\ \Omega$ yields

$$H(s) = \frac{10}{(s + 2.3)(s + 8.7)}, \tag{8}$$

so that there are two real poles at $s = -2.3$, $s = -8.7$.

Using Program TRESP in Appendix B to perform a simulation (see Section 3.3) yields the step response for $\omega$ shown in Fig. 2.6-2.

### b. Very Flexible Coupling Shaft

Coupling shaft parameters of $k = 2$ N-m/rad and $b = 0.2$ N-m/rad/s correspond to a very flexible shaft. Using these values, software like PC-MATLAB [Moler et al. 1987] can be employed to obtain the two transfer functions

$$\frac{\omega_m}{u} = \frac{20s[(s + 1)^2 + 4.36^2]}{s(s + 3.05)(s + 6.14)[(s + 3.4)^2 + 5.6^2]} \tag{9}$$

$$\frac{\omega_L}{u} = \frac{40s(s + 10)}{s(s + 3.05)(s + 6.14)[(s + 3.4)^2 + 5.6^2]} \tag{10}$$

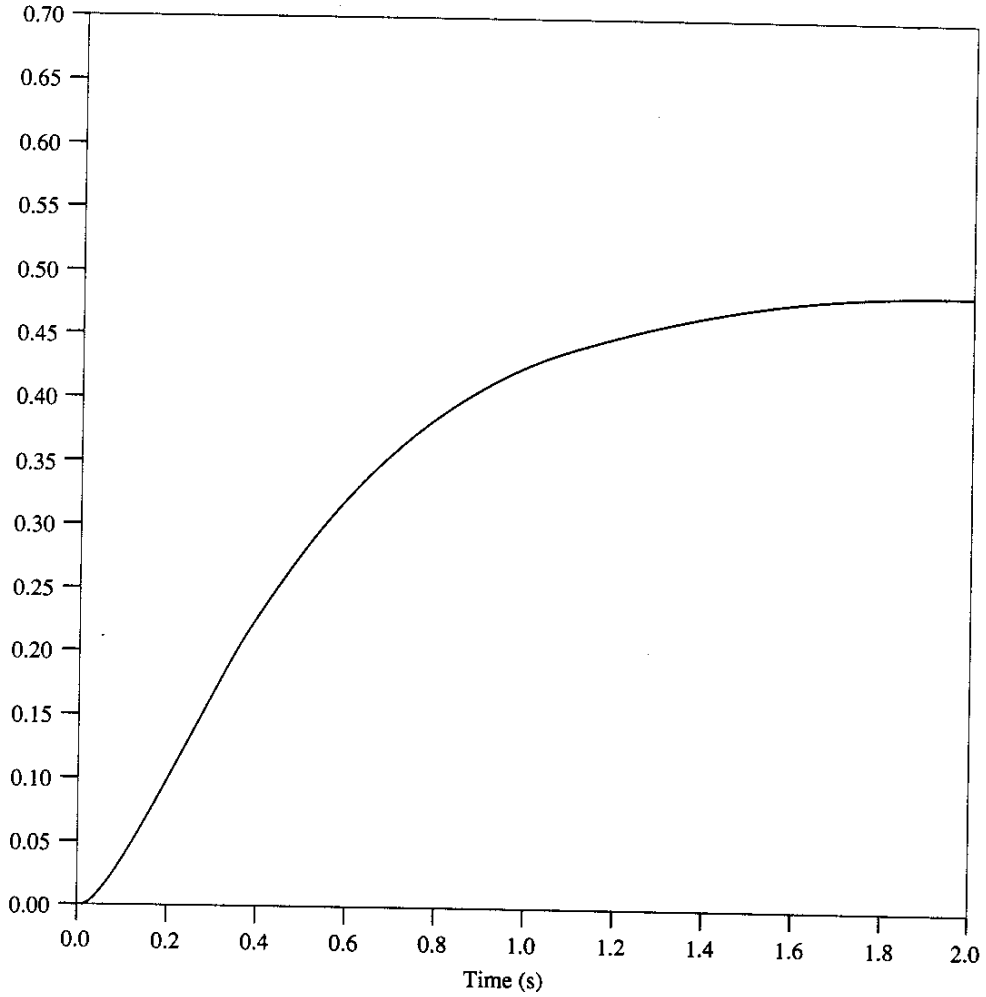



**FIGURE 2.6-2** Step response of dc motor with no shaft flexibility. Motor speed in rad/s.

The shaft flexible mode has the poles $s = -3.4 \pm j5.6$, and so has a damping ration of $\zeta = 0.52$ and a natural frequency of $\omega = 6.55$ rad/s. Note that the system is marginally stable, with a pole at $s = 0$. It is BIBO stable due to pole–zero cancellation.

Program TRESP yielded the step response shown in Fig. 2.6-3. Several points are worthy of note. Initially, the motor speed $\omega_m$ rises more quickly than in Fig. 2.6-2, since the shaft flexibility means that only the rotor moment of inertia $J_m$ initially affects the speed. Then, as the load $J_L$ is coupled back to the motor through the shaft, the rate of increase of $\omega_m$ slows. Note also that the load speed $\omega_L$ exhibits a *delay* of approximately 0.1 s due to the flexibility in the shaft.

It is extremely interesting to note that the shaft flexibility has the effect of speeding up the slowest motor real pole [compare (8) and (9)], so that $\omega_L$ approaches its steady-state value more quickly than in the rigid-shaft case. This is due to the "whipping" action of the flexible shaft.

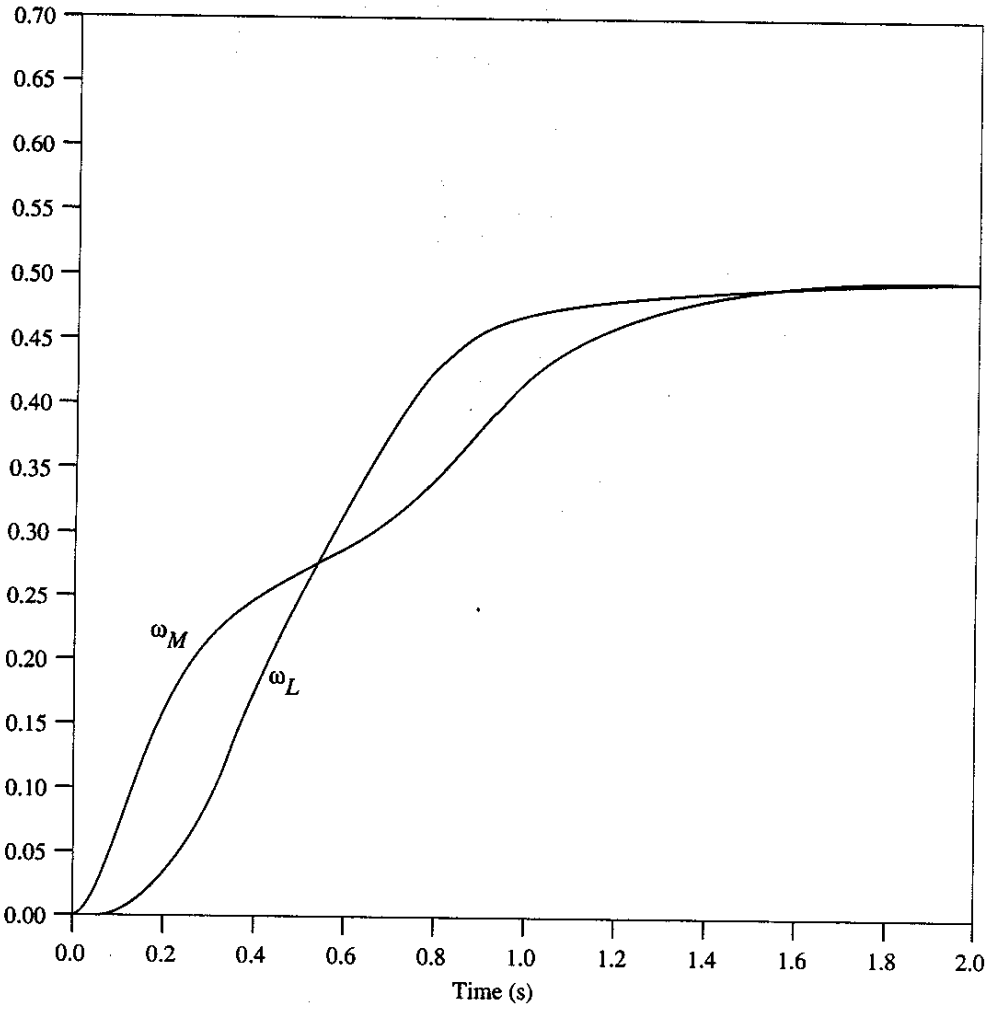



**FIGURE 2.6-3** Step response of motor with very flexible shaft.

The shaft dynamics make the control of $\theta_L$, which corresponds in a robot arm to the joint angle $q_i$, very difficult without some sort of specially designed controller.